Technical University of Denmark

DTU

Elements of extreme wind modeling for hurricanes

Larsen, Søren Ejling; Ejsing Jørgensen, Hans; Kelly, Mark C.; Larsén, Xiaoli Guo; Ott, Søren; Jørgensen, E.R.

Publication date:
2016

Document Version
Publisher's PDF, also known as Version of record

Link back to DTU Orbit

DTU Library
Technical Information Center of Denmark

Elements of extreme wind modeling for hurricanes

S. E. Larsen, H. E. Jørgensen, M. Kelly, X. G. Larsén,
S. Ott (DTU Wind Energy), E. R. Jørgensen (DNVGL)

DTU Vindenergi
E Rapport 2016

DTU Vindenergi
Institut for Vindenergi

Resume (mask. 2000 char.):
The report summarizes characteristics of the winds associated with Tropical Cyclones (Hurricanes, Typhoons). It has been conducted by the authors across several years, from 2012-2015, to identify the processes and aspects that one should consider when building at useful computer support system for evaluation hurricane extreme wind conditions for a given offshore site. It was initiated by a grant from DNV that has as well been represented by one of the authors in this report. Finally, we wish to emphasize the debt of this report to an earlier work at the DTU-Wind Energy Department on "Extreme winds in the North Pacific" (Ott, 2006).

Preface

The report summarizes characteristics of the winds associated with Tropical Cyclones (Hurricanes, Typhoons). It has been conducted by the authors across several years, from 2012-2015, to identify the processes and aspects that one should consider when building at useful computer support system for evaluation hurricane extreme wind conditions for a given offshore site. It was initiated by a grant from DNV that has as well been represented by one of the authors in this report. Finally, we wish to emphasize the debt of this report to an earlier work at the DTU-Wind Energy Department by another co-author: "Extreme winds in the North Pacific" (Ott, 2006).

DTU Wind Energy, 3 2016

Søren Larsen

Content

Summary

The report summarizes characteristics of the winds associated with Tropical Cyclones (Hurricanes, Typhoons). It has been conducted by the authors across several years, from 2012-2015, to identify the processes and aspects that one should consider when building at useful computer support system for evaluation hurricane extreme wind conditions for a given offshore site. It was initiated by a grant from DNV that has as well been represented by one of the authors in this report. Finally, we wish to emphasize the debt of this report to an earlier work at the DTU-Wind Energy Department by another co-author: "Extreme winds in the North Pacific" (Ott, 2006).

1.High wind cyclones

Tropical cyclones with wind speed exceeding about 40 m/sec are called Hurricanes in the Atlantic, while they are called Typhoons in the Pacific. Mid-latitude storms are strong winds associated with the frontal pressure systems there.
Tornadoes are also rotating wind systems, but are generally connected with outflows from thunderstorms, and of considerable smaller horizontal scale than the hurricane or the mid-latitude pressure systems. However, they do appear as well in connection with hurricane induced convection. Mid-latitude systems have a scale of 1000 km or more. The so-called polar lows are formed over the polar oceans, as a pendant to tropical cyclones. They are quite small, a few hundred kilometers, but often attain hurricane like winds (Rasmussen and Turner, 2003, Kristjansen and Kolstad, 2011). Hurricanes and Typhoons are in the size range 200km to more than 900 km, while tornadoes range from about 0.1-3 km across. The maximum wind speeds of the hurricanes and of the tornadoes are about the same, which can be experienced from the polar lows as well.
.

2. What is a hurricane?

From Ott; 2006, we cite: The western North Pacific wind climate is dominated by tropical cyclones, or typhoons as they are called in this part of the world. Tropical cyclones are the most devastating types of storms that exist on the planet, each year causing tremendous damage in terms of loss of lives and property. The purpose here is to estimate the implications for wind turbine design in the western North Pacific area, in particular as quantified by the fifty year wind.
Cyclones are circulating, low pressure wind systems. Extra-tropical cyclones (outside the tropics) are primarily formed at the interface between two air masses of different temperature, and the temperature difference between them is their main source of energy. The borders between the two air masses are characteristic cold and warm fronts that curl up around the centre. A tropical cyclone (TC) has a warm center surrounded by relatively colder air and there are no fronts. The energizing mechanism in TCs is the condensation of water vapor supplied by sufficiently warm sea surface. Rising, humid air causes the formation of intense, local thunderstorms which tend to concentrate in spiral shaped rain-bands; these can produce heavy downpours and winds as well as tornadoes. The central region is covered by a dense overcast, but just at the centre there usually is a circular spot, the 'eye', which is free of clouds, associated with the sinking air masses there. Inside the eye wind speeds are moderate and there can even exist a completely dead calm. This is in contrast

to the edge of the eye, the eye-wall, where maximum wind speeds are found, as well as the maximum updrafts. Figure 2-1shows a few satellite pictures of typical, fully developed tropical cyclones, while Figure 2-2 shows a principal overview of the cyclone. The eye, the rain bands and the overall circular structure is evident. Even if the individual thunderclouds inside the cyclone are highly irregular, turbulent and random, the overall, large scale, features of the flow appear regular and deterministic, especially near of the core region. This is revealed in greater detail by direct measurements, made e.g. by reconnaissance aircraft that are able to 'scan' the wind and pressure fields. The general pattern is a circulatory motion orbiting the eye resulting from a balance between the centripetal acceleration and a radial pressure gradient. Above a surface layer, the velocity generally decreases with height because the pressure gradient decreases. Near the surface the friction takes over causing the opposite trend so that the velocity has a maximum found typically at an elevation of about 500m. Below the velocity maximum friction makes the wind turn towards the centre, but near the eye-wall it is caught by a vertically spiraling jet extending 5-10~km up into the troposphere. At the top the jet 'spills over' and splits into an outgoing jet and a jet going back into the eye. The air inside the eye is therefore generally subsiding (descending) and flowing out towards the eye-wall along the surface. This explains why there are no clouds in the eye.
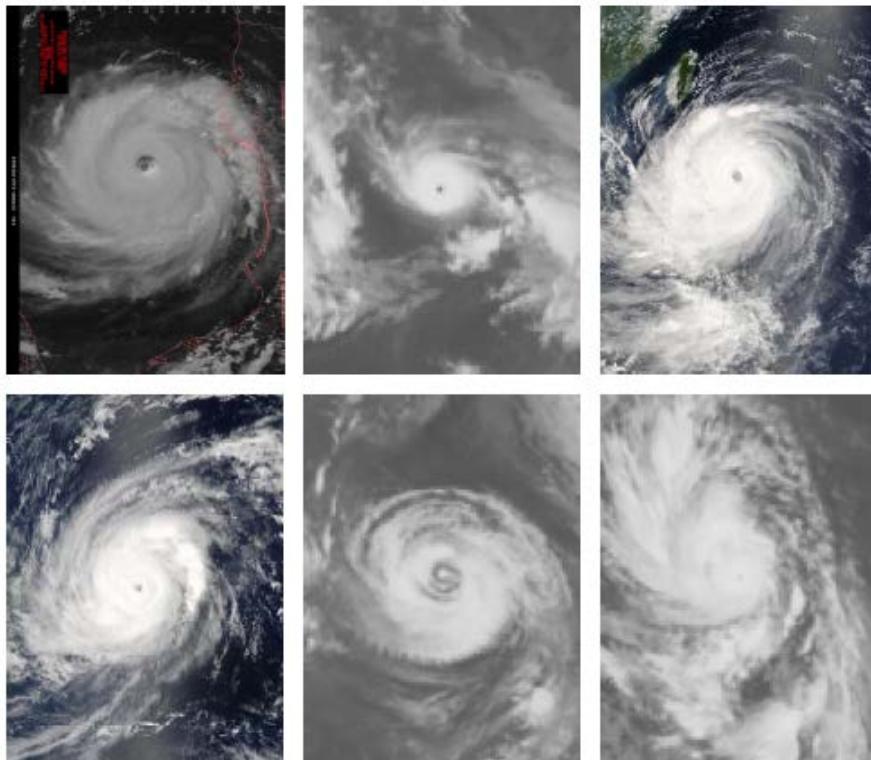
Figure 2-1 Images of fully developed tropical cyclones.(Ott,2006)

The mechanisms that control tropical cyclone genesis are not fully understood, so there is no explanation of why typhoons are particularly frequent in the

western North Pacific. It can be shown that tropical cyclones cannot form unless the sea temperature exceeds 26°C. In case of landfall the supply of water vapor is cut and the cyclone deteriorates rapidly, but it can still endanger a zone along the coastline several hundreds of kilometers wide. A warm sea is a necessary condition for tropical cyclone genesis, but it appears not to be the only condition. In fact there are major parts of the tropics, with plenty of warm sea, where tropical cyclones virtually never occur. These areas include the Eastern South Pacific, the South Atlantic (although a TC hit Brazil in March 2004) and a ten degree wide strip around the Equator where the Coriolis parameter is too small for TCs to form" (Ott, 2006).
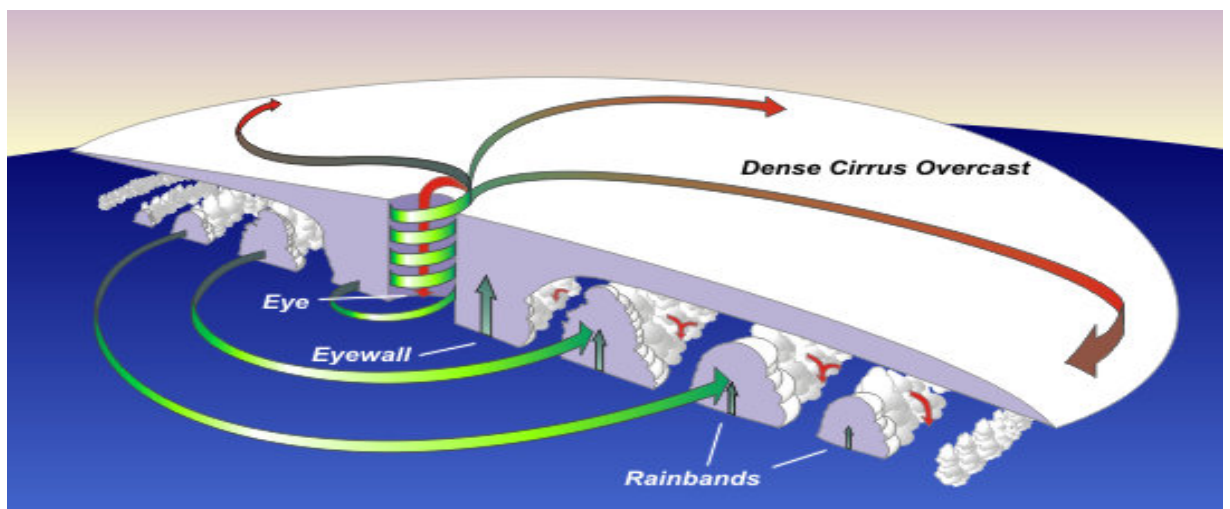
Figure 2.-2 Sketch of a tropical cyclone (Wikipedia)

2.1 When/where do hurricanes develop?

The hurricane (typhoon) formation areas appears from the figures below. Figure 2-3 records the hurricane track events from 1995-2006, while Figure 2-4 shows appearance from 1946 to 2006. Both figures are taken from Wikipidia. The main formation areas are seen to be close to but north of equator in the Atlantic Ocean and Pacific Ocean, and just South of equator in the Pacific Ocean. For both oceans the appearance is more frequent and stronger on the Western side of the oceans. One single hurricane has been recorded in the Southern Atlantic. In both figures the redder colors reflect more intensive hurricanes and the blue ones less intensive.
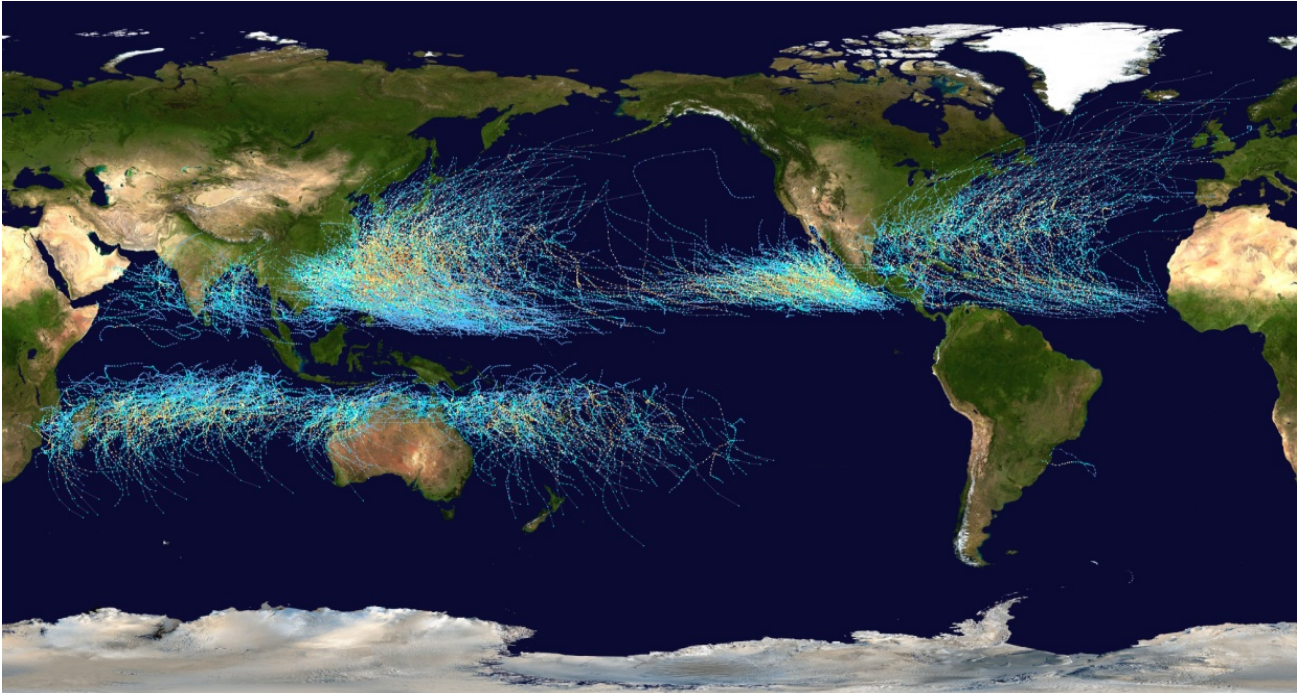
Figure 2.-3.Tropical Cyclones 1995-2006 (Wikipidia)

2.2 Differences between seasons and shore/offshore

Hurricanes (Typhoons) are exclusively formed over water, as described in the section about the process chapter, and they die fairly fast after having made landfall, because they loose their main energy supply from the water vapor condensation.   Most hurricane damage on shore is due both to wind loads and flooding. Additionally hurricanes can spawn tornadoes, especially during landfall, both at the right front quadrant and from meso-eddies within the eye. In general tornadoes can form over both land and water, but the most intensive tornadoes are found over land. Following WMO, sites more than 20 km off the coast can be considered "open sea". To what extent this describes as well hurricane situations is somewhat uncertain (ABS, 2011).

Worldwide the tropical cyclone activity peaks in late summer, where the differences between temperature aloft and the sea surface are the greatest. However, each particular basin has its own seasonal pattern. Tornadoes are most common in spring and least common during the winter.

Figure 2-4 Tropical cyclones 1945-2006 (Wikipidia)

3. Wind characteristics of hurricanes.

Extreme wind speed (averaging time and period of occurrence).
Evaluation of the extreme winds for hurricanes can conveniently be broken into two parts: (a) the physical distribution of winds across a hurricane, and (b) the probability for hurricane occurrence, strength and size, where such climatology is dominated by hurricanes, roughly corresponding to the track maps presented in section 2.

For the physics, we shall refer to the so- called Holland model (Holland 1980, Harper and Holland, 1999). It is based on a balance between the pressure gradient, the gradient wind and the Coriolis force, Derivation and details about the distribution and its validity is given in Ott (2006) that is appended to this report. From Ott (2006), we cite the simplified equations and the characteristics of the wind distribution, the Holland curve:

$$V_g^2 = \frac{r}{\rho}\frac{\partial P}{\partial r} - frV_g \Rightarrow V_g = -\frac{fr}{2} + \sqrt{\left(\frac{fr}{2}\right)^2 + \frac{r}{\rho}\frac{\partial P}{\partial r}} \qquad (3\text{-}1)$$

Where V_g, denoted the gradient wind, is the radial wind balancing the Coriolis force and the pressure gradient at distance r from the center. Ott (2006) uses the ratio between the surface wind (at 10m) and V_g to be approximated as 0.7.

The resulting wind speed as function of r is seen in below

Holland Model
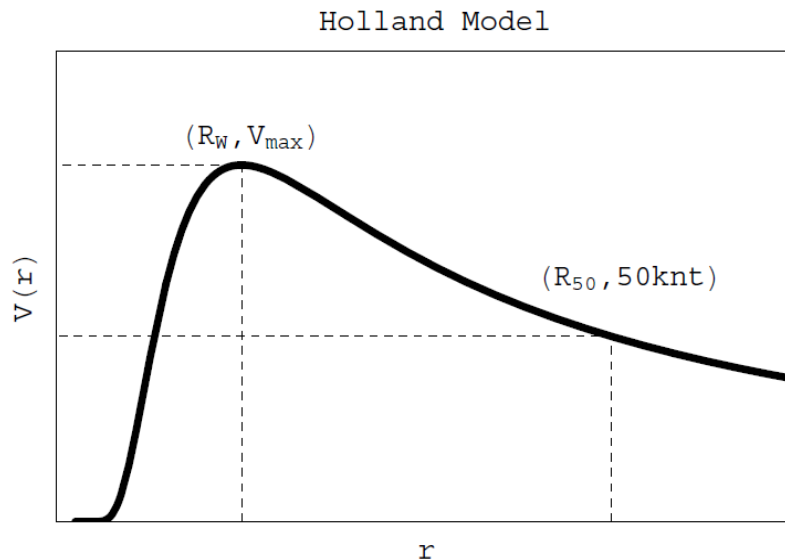
Figure 3-1 The Holland curve for the radial distribution of the horizontal wind in a hurricane (Ott, 2006).

V_{max} is called the maximum sustained wind and is correlated with the pressure depression in the eyeball of the hurricane. V_{max} (or pressure depression) and the two radii R_W and R_{50knt} now approximate strength and dimensions of the hurricane, see further discussion in Ott (2006). It is seen that V_{max} is the maximum wind charactering the hurricane. Rather than corresponding to a specific spatial average, it is a wind speed parameter. The averaging time corresponding to V_{max} for a stationary sensor will dependent on the advection speed and direction of the hurricane. But one will normally assume that the maximum of a 10-60 min average speed corresponds to V_{max} . For lower averaging times, of the order of seconds, one will have to consider a gust value of the wind, which shall be considered later.
The Holland model can be updated and improved somewhat, e.g. relaxing the axial symmetry as proposed in Emanuel (2004). However, the Holland model is not considered substantially incorrect, and it is found to reproduce data with a mean bias within 1 m/s (Ott, 2006).

Model Estimates based on pressure rather than on wind speed
The relation between pressure and wind, depicted by equation (3-1) indicates that either pressure or wind field can be equally well used to describe a hurricane. However, in practice the correlation between the pressure depression and maximum wind speed is less than perfect (Ott, 2006), which means both approaches demand further modeling to estimate the hurricane

wind field. Specifically, the observational problem of determining how close the observations get to the center of the hurricane is similar for both variables. According to models about hurricanes, as described above, the horizontal characteristics of the hurricanes are to a large extent described by the pressure at the center and ambient pressure: Following simple models one can hereafter estimate the radius to the maximum wind, R_w, and the maximum wind, V_{max}, itself, provided one knows the shape of the wind distribution, which does not derive from the above parameters in an easy way. Therefore one typically estimates the radius to where the wind is 50 knt, R_{50}, *to* describe the extend of the hurricanes. Additionally the advection velocity, and indeed the track history becomes of importance to translate the hurricane characteristics into estimates of the extreme wind climate. This is considered in more detail in section 6.

3.1 Horizontal winds from hurricanes.

At any given location, the probability function for the extreme winds associated with hurricanes can be determined from a combination of the wind distribution for each hurricane at each time step, combined with its probability of occurrence of this particular hurricane at the location considered. Hence, one will have to consider a multivariate distribution function and from this derive the extreme wind variable considered, for example as the 50 or the 100 year wind.
The simplest method is to start by considering the probability of occurrence of certain classes of hurricanes from the track records presented in section 2-2, and thereafter continue to consider the wind characteristics for these classes using wind distributions as the Holland distribution, in Fig. 3-1. Detailed methods will vary with the parameters that need to be discussed. Unfortunately, the methods must also be dependent on the available data, and not all the hurricane data available at the data centers include enough information to describe the path, size and strength of each hurricane. See discussions in section 6.

3.2 Wind direction changes due to hurricane advection.

The wind direction changes can be either turbulent or reflect the larger scale wind direction changes induced by the hurricane advection. E.g. a wind turbine site may experience the wind in the eye-wall, thereafter the calm in the eye, followed by the eye-wall winds on the other side of the eye. The rate of this transition is controlled by the advection speed of the cyclone. Ott (2006, p 18) presents data and an analysis indicating that the horizontal wind direction change should be within 0.1 °/sec, while the wind speed change is within

2m/s/min. However, he points out that these estimates are based on hurricane data, while a tornado created from the hurricane would considerably increase the changes in wind.

A change in vertical wind is experienced also when the wind turbine is confronted by passage of the eye wall, with a transition from maximum upward vertical wind speed to descending air within the eye, or back. Again the advection (hurricane 'translation') speed becomes the controlling factor. Measurement of vertical winds in hurricanes are not very plentiful, however, some model outputs are available, e.g. (Smith and Thomsen, 2010). Here, maximum updrafts occur within the eye- wall, at heights between 1 km and 10 km. The lower maximum around 1 km is 1-2 m/s, dependent on boundary layer parameterization, similarly for the model case, V_{max} is about 70 m/s also 1 km over the surface. Taking the 2 m/s, with a linear decrease towards the surface, this corresponds to 0.4 m/s at 200m. Assuming that w/w_{max} changes as V/V_{max}, we refer to Ott (2006) as for the horizontal wind changes, and find that the vertical wind speed rarely changes more than 1 cm/sec per 10 min. As for the horizontal changes, one will also for the vertical changes have to consider the possibility of tornadoes riding on the eye-wall, creating larger small scale change in the vertical velocity.

3.3 Wind speed in the eye of the hurricane.

The eye of the hurricane is normally characterized by calm conditions and sinking air, also within the eye the wind profile is close to logarithmic in the lowest few hundred meters. In spite of the low wind speed the water surface is quite rough, due to the distorted surface wave fields (Makin, 2005)

3.4 Wind shear and wind profile.

Examples of shear are shown in Figure 3.-2. The logarithmic wind profile is found exist up to several hundred meters, in consistency with other authors (Zhang, 2011), who reports logarithmic wind profiles to exist up to about 500 meters in between the rain bands in the outer vortex. The low value of z_0 used in spite of the very high wind speed in the eyewall is consistent with new models for z_0 and surface drag as function of wind speed, as discussed below. Hence, we expect the wind shear in the lowest few hundred meters to be consistent with the logarithmic profile, using the Charnock's relation for z_0 for wind speeds up to about 30 m/s, where a gradual decrease of z_0 with wind speed will set in; this follows data from Powell et al (2003) and the theoretical explanation of Makin(2005), see Figure 3.-3 .

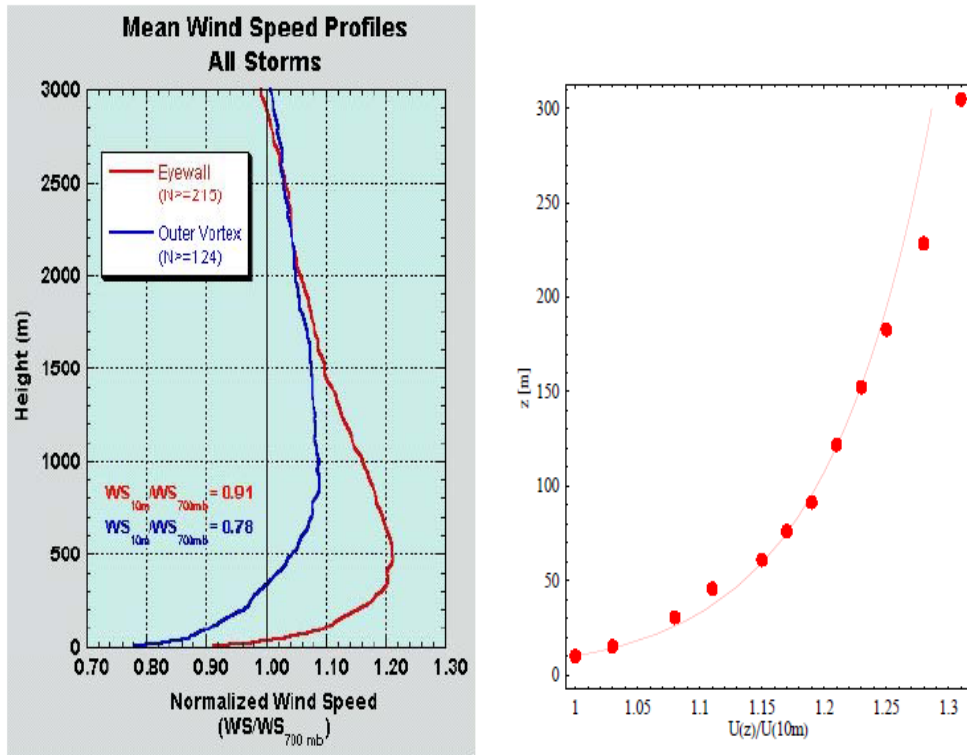*Figure 3.-2. Left: Hurricane wind profiles obtained by GPS drop-sondes. The wind speed at 700mb is used as reference, since this is typically measured from aircraft. Right: Eyewall data, plotted together with a logarithmic profile where $z_0 = 0.07$ mm (Franklin, Black and Valde, 2000).*
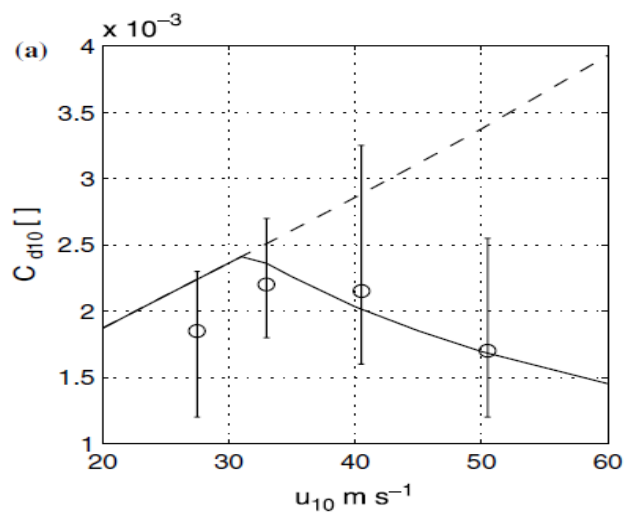

Figure 3.-3. The surface drag coefficient according to Charnock's relation (broken line) and according to Makin (2005).

4. Turbulence (spectra, coherence, intensity and length scales)

Based on airplane data between the surface and 400 m within hurricanes, Zhang (2011) found that the shapes of dimensionless turbulence power spectra and co-spectra generally resemble the shapes of those from earlier studies (e.g. Kaimal et al., 1972), but shifted to higher normalized frequencies ($n = fz/U = z/\lambda$, corresponding to smaller wavelengths). Peak normalized frequencies of the u-spectra are roughly 0.05–0.2 and the w-spectra have peaks at about 0.2–0.3; this is a relatively small difference between the u- and the w-spectra, as opposed to results for standard boundary layers (Kaimal et al, 1972) where the corresponding values are 0.05 for the u- and 0.5 for the w-spectrum. Additionally Zhang *et al.* (2009) and Zhang (2011) found surface-layer scaling of variances and spectra valid up to $z \sim 500$ m. This is consistent with the logarithmic behavior of the wind profile in the 'outer vortex' shown in Figure 3-2 (Powell *et al.*, 2003). The figure also includes a logarithmic profile is plotted over wind profile data from the eyewall, where the logarithmic behavior has a vertical extent that is clearly smaller than for the profile in the outer vortex.

It should be emphasized, however, that there is not yet (as of 2015) a consensus about turbulence statistics within hurricanes (e.g. Smith and Montgomery, 2010; Lorsolo *et al.*, 2010). Close to the surface, Yu *et al.* (2008) (from data at heights mostly below 10 m) find characteristics that are different from that reported by Zhang *et al.* (2011).

Due to the evidence that hurricane boundary layer wind statistics behave (to low order) much like those in a conventional surface-layer, we begin to describe the turbulence part of the hurricane problem by estimating a range of spectral expressions to be used within the Mann (2001) spectral system. The Mann model is then employed to simulate time-series that can be used in horizontal axis wind turbine (HAWT) models.

Here we use the recent spectra by Zhang (2011) - whose non-dimensional forms collapse together - measured during two hurricanes as part of the CBLAST experiment, and taken by aircraft flying in stepped descents ranging from 69–374 m. French *et al.* (2007) provide details of the measurements and more wind statistics.

Given the mean dimensionless spectra provided by Zhang (2011), one may fit the IEC-accepted three-dimensional spectral-tensor turbulence model of

Mann (1994) to obtain representative parameters needed to simulate turbulence in the hurricane boundary layer. Doing so, for an effective height of ~200 m and wind speed of ~30 m/s we find a fit (as shown below) which results in values of the Mann-model length scale L=100 m, anisotropy parameter Γ=3.1, and normalized dissipation rate $\alpha\varepsilon^{2/3} = 0.015$.
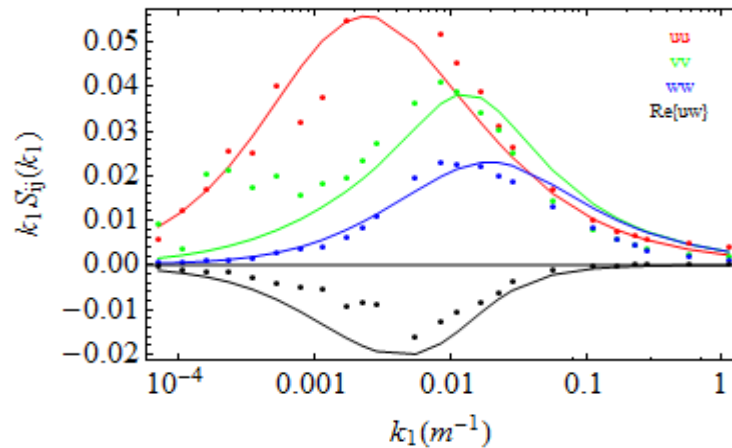
Figure 4.-1 Match of the Mann (1994) spectral model (curves), to the hurricane data (points) of Zhang (2011).

The relatively small length scale $L \sim 100$m (for a mean height of roughly 200 m) reflects the findings of Zhang (2011) that the horizontal spectral peaks occur at smaller scales than predicted by the classical spectral forms of e.g. Kaimal (1972), and also with the existence of a deepened surface layer extending beyond 400 m. The variation in wind speeds and heights within the exploited dataset lead to a range of spectral amplitudes and consequently range of Mann dissipation parameter, $\alpha\varepsilon^{2/3}$, but cause relatively little variation in characteristic length scale L or anisotropy parameter Γ; conservative estimates (using ±0.2 m/s for the friction velocity; see French *et al.,* 2007) lead to a variation in the spectral amplitude of ±0.005 (~30%) for $\alpha\varepsilon^{2/3}$. The same basic results were obtained using the Charnock parameterization with friction velocity and estimated mean height (from French *et al.,* 2007), since at these wind speeds Charnock's relation is still expected to predict effective roughness.

In comparison, data from the Great Belt Experiment (essentially over-sea, with z=70m and U=22m/s) gave larger spectral amplitudes ($\alpha\varepsilon^{2/3}$ ~0.1), but with commensurate L=61m (since L scales with z) and a similar Γ of 3.2 (Mann, 1994). Regarding the value of Γ=3.9 in the IEC standard, it should be noted that this larger value is based on old data at lower wind speeds (Mann, 1998). Similarly, analysis of the spectra provided by Yu (2008) implies an unrealistic value of Γ=5, due to the data being taken at only 10 m height. For heights relevant to wind turbines, a value of Γ near 3 is expected in the hurricane

boundary layer, as found here and in Mann (1994); further, more recent analysis has shown that for heights above 60 m, $\Gamma \to \sim 3$ (Peña *et al*, 2010; Dimitrov *et al*., 2015).

It may be worth mentioning that section 4 of the ABS(2011) discusses the difference between the turbulence modeling within the API (2007) or so-called Frøya wind spectrum, and the IEC (2009) report which follows mainly the Kaimal spectrum. The Frøya spectrum has more low frequency and less high frequency energy than the Kaimal spectrum. ABS (2011) considers the issue as unresolved. Here we point out that the spectral form proposed by Zhang (2011), and studied here, has even less low frequency energy than the Kaimal-spectrum.

4.1 Turbulence (peaks and gust factors).

One may estimate the peak factor $k_T = \left(\left\langle U_{\max} \right\rangle - \left\langle U \right\rangle \right) / \sigma_U$ via

$$k_T = \sqrt{2 \ln \left(\frac{T_0}{2\pi} \sqrt{\frac{m_2}{m_0}} \right)}, \qquad (4.\text{-}1)$$

where T_0 is the duration of turbulence measurements, and σ_U is the variance of u, using the moments

$$m_j = 2 \int_0^\infty \phi^2(\omega)\omega^j S(\omega)d\omega \qquad (4.\text{-}2)$$

of the filtered power spectrum *S(ω)* of *u* (assuming a Gaussian process), ω is the radial frequency and $\phi(\omega) = \mathrm{sinc}\left(\omega T_a / 2 \right) = \sin\left(\omega T_a / 2 \right) / \left(\omega T_a / 2 \right)$ is a filter accounting for the temporal resolution with averaging time T_a.

Unfortunately the CBLAST hurricane spectra from Zhang (2011) alone cannot be considered reliable for calculating k_T based on typical 10-minute averages, due to the short duration (2-3 minutes) of the measurement records. While the formulation (4-1) with standard filtering time T_0 = 10 minutes appears to give reasonable peak factor values, consistent with the range prescribed by ESDU (1983) and the gust factor findings of Vickery and Skerlj (2005), k_T is sensitive to the filter prescription—and particularly the averaging time. Using $T_a = 10$ minutes filters away much of the CBLAST data signal, and thus reasonable results should not be expected from the CBLAST spectra for T_a larger than 1–2 minutes. However, using the Mann (1994) model with fitted parameters corresponding to the CBLAST hurricane spectra (*L*=100 m, Γ=3.1, $\alpha \varepsilon^{2/3} = 0.015$ as above), but over a wider range of wavenumbers, provides more reliable results. Doing so produces k_T of roughly 4.3–4.5, matching the

Kaimal (1972) result for L=100 m; the smaller effective length scale leads to a small increase in k_T of <~0.5%. Both spectral forms lead to only a weak dependence on wind speed through the collapse of the spectra to non-dimensional form $S(fz/U)$, with k_T rising only 1% for wind speeds increasing from 20 to 60m/s.

The gust factor G can be found from the peak factor, as $G = 1 + k_T I_U$ where $I_U = (\sigma_U/\langle U \rangle)$ is the turbulence intensity. Using Kaimal- (or Mann-) spectra to calculate σ_U along with the k_T found above, one obtains results similar to Wang *et al.* (2010) and with the same range as Vickery & Skerlj (2005), shown in Figure 4-2. However, Vickery & Skerlj (2005) found a slight increase of G with U, due to the effect of increasing surface roughness offsetting the otherwise decreasing $G(U)$; the empirical ESDU form also prescribes an increase in G with U over water. The reduction in length scale observed e.g. in CBLAST translates into a gust factor reduced by ~10% (solid line versus dotted line), while further modifying that result with a correction factor $(m_0)^{1/2}$ for averaging time (empirically set in ESDU and mis-expressed as m_0 in Balderrama *et al.,* 2012) leads to the mixed result shown by the dashed line in the Figure 4-2.
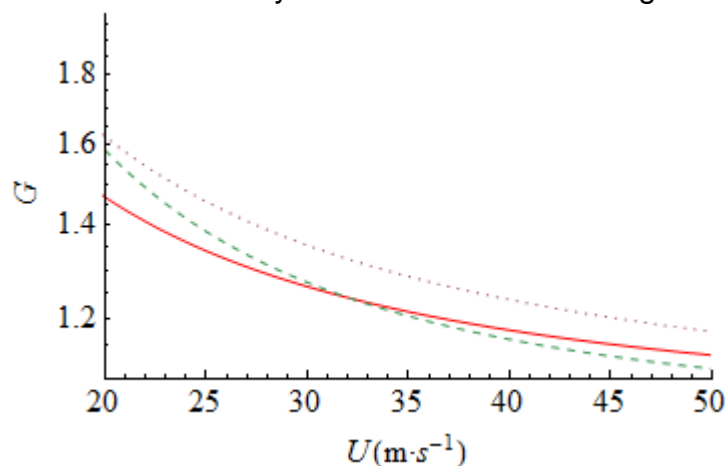
Figure 4.-2. Estimated hurricane gust factor versus mean wind speed using spectral modeling with parameters corresponding to CBLAST data fits. Dotted: *L*=210m, solid: *L*=100m, dashed: *L*=100m plus averaging-time correction.

Data from a much larger number of cyclones have been used by e.g. Yu (2008) and Balderrama *et al.* (2012) to provide analysis useful for loads on buildings, but these give estimates of gust factor not applicable to wind turbines due to the sensors being unrepresentatively close (10 m) to the surface. We also note that spectral moment results should be taken with caution (see Ott *et al.*, 2005) due to the (potentially) non-Gaussian character of the wind fluctuations; though Balderrama *et al.*(2012) found the non-Gaussian peak factor method of Kareem and Zhou (1994) to be useful at least for near-ground measurements. Further,

the low-wavenumber shape of any spectral form (e.g. Mann spectral tensor, Kaimal, ESDU) is a source of uncertainty.

The estimated turbulence intensities gust factor can also be estimated by considering the peak and gust factor forms above; these lead to a linear dependence of I_U upon $U_{\max}$, which are confirmed by DNV data as shown in Figure 4.-3.
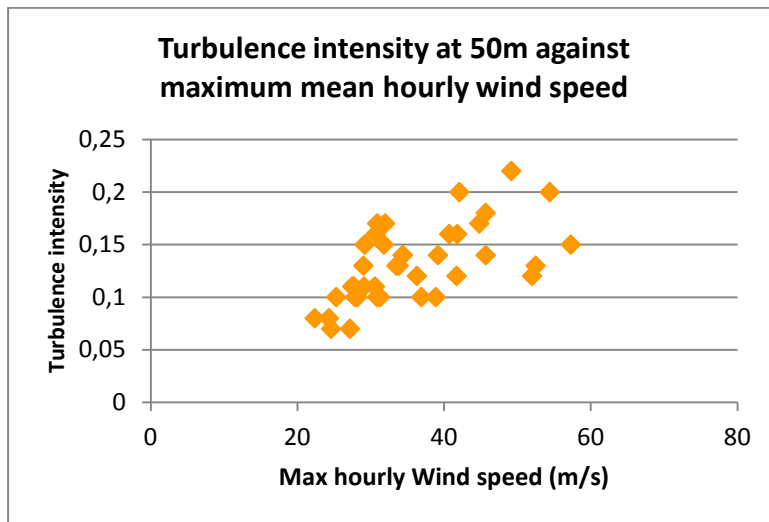
Figure 4-3. Measured hurricane turbulence intensity versus maximum hourly mean wind speed from Typhoon measurements (DNV Denmark, 2011)

More data needs to be analyzed at a number of heights and speeds, including individual (e.g. CBLAST) transects as well as high-wind data (e.g. Høvsøre and elsewhere), to further clarify the variability in turbulent spectra, associated model parameters, and additional wind-speed dependence. The issue of gust factors needs to be revisited using better data, and is a current topic of research at DTU Wind Energy.

5. Centers for historical data of tropical cyclones.

Historic typhoon data available from these sources are in the form of so-called 'best tracks' or HURDAT for the North Atlantic region. These are constructed on the basis of all available information, hind casting rather than forecasting. The amounts of detail given in track records vary, but as a minimum they contain the center position and central pressure (at sea level) at 6 hours interval. This database is utilized for a wide variety of purposes: setting of appropriate building codes for coastal zones, risk assessment for emergency managers, analysis of potential losses for insurance and business interests, intensity

forecasting techniques, verification of official and model predictions of track and intensity, seasonal forecasting, and climatic change studies.

5.1 Best track hurricane data from different regions.

The following list provides links to where Best Track Data for each region may be obtained:

1. HURDAT for Atlantic region from NHC (1851-2011) :
   http://www.nhc.noaa.gov/data/hurdat/tracks1851to2010_atl_2011rev.txt
2. HURDAT for Eastern North Pacific region from NHC (1949-2009) :
   http://www.nhc.noaa.gov/data/hurdat/tracks1949to2010_epa.txt
3.
4. http://www.nhc.noaa.gov/data/hurdat/tracks1949to2010_epa.txt
5. JTWC Northern Indian Ocean Best Track Data (1945-2010) :
   http://www.usno.navy.mil/NOOC/nmfc-ph/RSS/jtwc/best_tracks/ioindex.html
6. JTWC Western North Pacific Best Track Data (1945-2010) :
   http://www.usno.navy.mil/NOOC/nmfc-ph/RSS/jtwc/best_tracks/wpindex.html
7. JMA Best Track Data for Western North Pacific Ocean and South China Sea (1951-2011):
   http://www.jma.go.jp/jma/jma-eng/jma-center/rsmc-hp-pub-eg/trackarchives.html
8. IMD Best Tracks Data for Bay of Bengal and the Arabian Sea (1990-2009) :
   http://www.imd.gov.in/section/nhac/dynamic/bestrack.htm

Best track data are available from the International Best Track Archive for Climate Stewardship (IBTrACS). Link: http://www.ncdc.noaa.gov/oa/ibtracks/.

The archive contains best track data from 12 different agencies and covers all basins where TCs occur. There are some differences with respect to the parameters contained in the data. All list centre position, central pressure and a maximum wind speed, but a parameter indicating the size of the cyclone is not always given.
In principle best track data represent the best guess that can be made in hindsight taking all available information into account. These could be either output from forecast models (run in hind-cast mode) or observations from ships, aircraft reconnaissance or satellite measurements and images. However, in almost all cases the best track data are derived from satellite images using the Dvorak method. This is a technique which correlates certain geometric features of the images with measures of storm intensity. The image analyst follows a set of well-defined rules, and ends up with an intensity number. By means of a table

this number is then converted to specific values for central pressure depletion and maximum sustained wind speed. Indirectly this postulates an absolutely perfect correlation between pressure and maximum velocity, which is a huge simplification of reality. It should be noted that different sets of rules different and different 'perfect' pressure-velocities correlations are in use by the different agencies. This can lead to conflicting results. Thus for the western North Pacific, covered by JMA, Shanghai Typhoon Institute, the Hong Kong Observatory and JTWC, there exists a discrepancy between JTWC and the three other agencies (JTWC wind speeds are considerably higher than for the other agencies). These matters are further discussed in Ott(2006).
A number of marine network and buoy sites on the US East Coast, in regions where the extreme winds are hurricane determined, have been in operation for sufficient time to allow a standard Gumbel estimation of the 50 and 100 year values of wind and wave height to be employed (ABS, 2011, p 34). Additionally, the data should provide good validation data for models of hurricanes hitting the US East coast and Gulf of Mexico. For winds a problem can be the often very low measurement heights.

5.2 Hurricane wind data from JMA and JTWC.

The Best Track Data from JMA and JTWC have a varying amount of details, but as a minimum, they contain the center position and the central pressure (at sea level) at 6 hours intervals ,see table 5.-1.

Parameters	Unit
Time of Analysis	yy/mm/dd/hh
Grade/Intensity	Dimensionless
Center Latitude	Degree
Center Longitude	Degree
Central Pressure	hPa
Max. Sustained Wind Speed	Knots
Longest radius direction (30 & 50 kt winds)	Degree
Radius (30 &50 kt winds or greater)	km

Table 5.-1. Information provided by JMA and JTWC.

In order to do extreme wind analysis, size information is required. As can be seen from table 5.-1 the central pressure, maximum sustained wind speed, and direction radius are provided in the JMA best track data. Only wind speeds exceeding the cut-off value 50 knots = 25.7 m/s should be kept, as this refers to the limit utilized by JMA to qualify a tropical cyclone as a typhoon.

Elements of extreme wind modeling for hurricanes

6. Statistical estimation of extreme winds for regions with hurricanes.

The estimation of hurricane extreme winds involves a combination of two methodologies, a model to get from observed wind to the maximum wind occurring close to the eye of the hurricane, and an extreme value statistical method that from observations allow one to estimate the extreme winds (at low probabilities, the 50 year wind-say).

6.1 Direct estimation from best track data.

The simplest method is to start by considering the probability of occurrence of certain classes of hurricanes from the track records presented in section 2.2.-1, and thereafter continue to consider the wind characteristics for these classes using wind distributions as the Holland distribution, in Fig. 2.3-1. Detailed methods will vary with the parameters that need to be discussed. Unfortunately, it must vary too dependent on the available data, and not all the hurricane data available at the data centers include enough information to describe the path, size and strength of each hurricane.

A method has been developed in Ott (2006) that is appended here. The method was originally based on analysis of satellite images. This method correlates certain geometric features of the images with measures of storm intensity. Ott (2006) creatively used this method for obtaining the extreme winds in the Pacific Ocean, applying a modified Gumbel statistical method.

It is the "best track" data that are used in connection with this method to estimate wind series . The extreme winds in the Western North Pacific Ocean are dominated by tropical cyclones (typhoons). Each year between 1951 and 2004, the Japanese Meteorological Agency (JMA) issued official best track data in this region based on center positions at 6 hours intervals along with the characteristics such as central pressure, maximum sustained wind speed and size indications. Using a simple, analytical model it is then possible to derive a velocity field on the center and derive wind speeds at a specific location for each individual typhoon, using the Holland model in Fig.3-1. Hence it is possible to derive hurricane generated wind time series for any point within the hurricane area considered For the JMA the area is North of equator and between 100 E and 180 E. These wind time series can now be the basis for extreme value estimation, using standard techniques to estimate expected extreme winds (like U_{50}) from time series, see Ott(2006), using Gumbel distributions etc. Figure 6-1 illustrates the resulting U_{50} isoline plot.

Similar "best track" data may be available from other sources and areas, but they have so far been difficult to identify. However, if identified, the approach of Ott (2006) is possible to be applied to other areas of the global oceans.
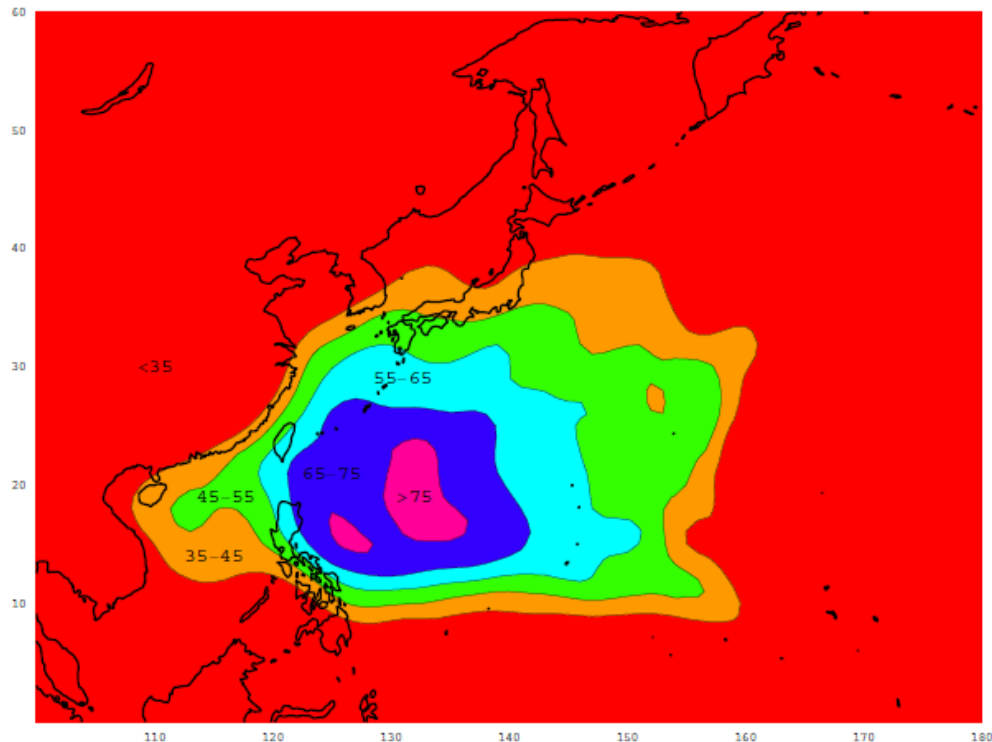
Figure 6-1 U_{50} (m/s) from JMA best tracks for Western North Pacific, based on the satellite images of the Typhoon (Ott, 2006).

A number of marine network and buoy sites on the US East Coast, in regions where the extreme winds are hurricane determined, have been in operation for sufficient time, > 10 years, to allow a standard Gumbel estimation of the 50 and 100 year values of wind and wave height to be employed (ABS, 2011, p 34). For winds a problem can be the often very low measurement heights.

6.2 Meso-scale modelling from reanalysis data, applying spectral correction.

As an alternative to use the "best track" records, one might consider using available Reanalysis Data to establish the wind climate record necessary to estimate the extreme winds, like U_{50y}. This on the other hand necessitates use of mesoscale modeling with corrections to resolve the hurricanes to resolve the high winds. Two methods are described below:

6.2.1 The data

The global reanalysis data from NCEP/NCAR reanalysis II (NRA II, 1979 - 2011) and the global Climate Forecast System Reanalysis data (CFSR, 1979 - 2010) have been investigated for calculating the extreme wind, in connection with the application of the spectral correction method (Sec. 6.2.2) (Larsén et al. 2013a, 2014). The NRA II data are 6 hourly and have a horizontal resolution of

about 200 km and the CFSR data are hourly and have a horizontal resolution of about 40 km. From NRA II data, the pressure and temperature data were used to calculate the geostrophic wind and extract the geostrophic wind to the wind of the standard condition, e.g. at 10 m, over homogeneous surface of roughness length of 5 cm. From the CFSR data, the surface wind records were used.

6.2.2 The downscaling method

This is a statistical downscaling approach to "correct" the data from global reanalysis data to match the measurements with the mesoscale variability in terms of the power spectrum. The modeled data introduced here are of the horizontal resolution of approximately 200 km and 40 km, one value every 6 hours and 1 hour, respectively. If we use these data directly, the extreme winds will be severely underestimated caused by the smoothing effect of the effective resolutions of the models (Larsén et al. 2011). The smoothing effect is reflected as energy deficit or missing power spectral energy in the mesoscale range, compared to that of the measurements. The difference in the measured and modeled power spectrum can be seen in Figure.6-2, where the power spectra of several mesoscale modeled wind time series are plotted together with the spectrum from measurements.
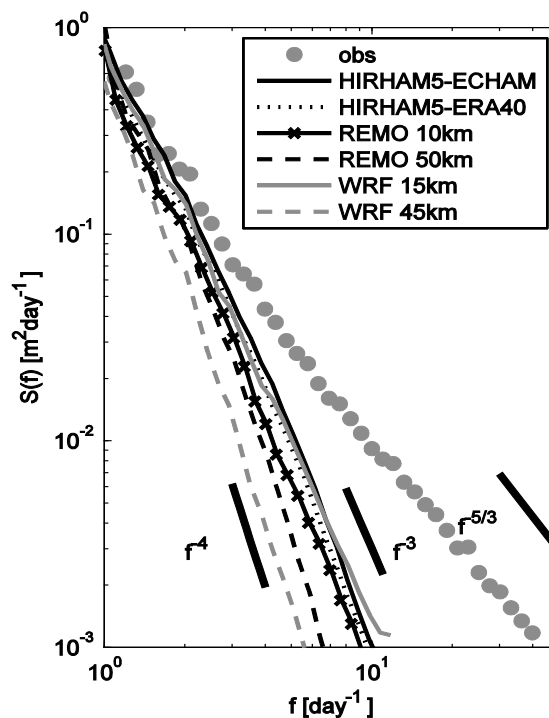

Figure 6.-2 Wind speed power spectra from several mesoscale models and from measurements (gray dots).
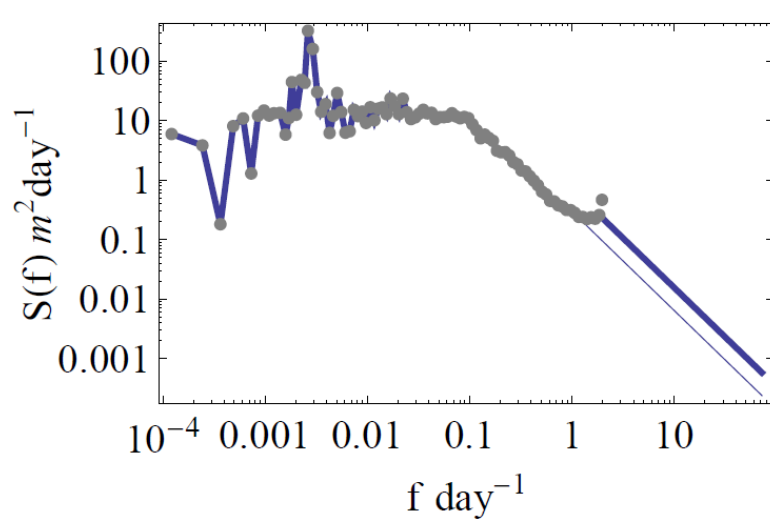
Figure 6-3 Power spectrum of the standard wind from NCEP/NCAR reanalysis data II at a NCEP/NCAR grid point (25.7N, 127.5E) (gray dots). The blue curves extend the spectrum from f=1 day^{-1} (thin) and 1.8 day^{-1} (thick) respectively to 72 day^{-1}.

The details of this spectral correction approach can be found in Larsén et al. (2011). To briefly describe the method: we modify the power spectrum of the time series of the modeled data to match that expected of measurements and extend the power spectrum from the Nyquist frequency of 6 hours to 10 min. Figure 6.-3 shows the power spectrum of the reanalysis data at Nyquist frequency of 2 day^{-1}, the gap between the reanalysis data and a mesoscale resolution of 10 min is filled in by the thick blue curve at 1.8 day^{-1}. The thin curve shows a selection of the spectral correction at another frequency of 1/ day. The zero- and second order moments of the power spectrum, m_0 and m_2, are thus corrected and will be used to calculate the smoothing factor of the mean annual maximum wind and eventually the 50-year wind. The main algorithms are given below:

$$k_T = \frac{\overline{U}_{max} - \overline{U}}{\sigma_U} = \sqrt{2\ln\left(\frac{T_0}{2\pi}\sqrt{\frac{m_2}{m_0}}\right)}$$
(6.-1)

where

$$m_j = 2\int_0^\infty \phi^2(\omega)\omega^j S(\omega)d\omega$$
(6.-2)

with $S(\omega)$ the power spectrum of Gaussian process, ω is the radian frequency and $\phi(\omega) = \sin(\omega T_a / 2)/(\omega T_a / 2)$ is a filter accounting for the temporal resolution with averaging time T_a. T_0 is the basis period of 1 year. Note, the completely similar equations of (4.-1) and (4-2), but here T_0 is 1 year and T_a is our resolution averaging time.

Elements of extreme wind modeling for hurricanes

It is expected to study in more depth the spectral behavior of hurricane case in order to improve the application of this method by exploring many reanalysis data.

The Annual Maximum Method is used to calculate the 50-year wind. The winds of the standard conditions and those over the actual water surface roughness can be transformed.

6.2.3 Storm episode method using hurricane forecasting and mesoscale modeling.

In this method, over a certain area, all hurricanes during a long enough period should be simulated using mesoscale modeling. For each mesoscale grid point, the annual maximum winds from the simulated hurricanes can be used to calculate the 50-year wind. The details of applying the downscaled storm episodes to calculate the 50-year wind for a particular region can be found in Larsén et al. (2013b)

In order to have the simulated hurricanes samples, a shortcut is to obtain the finished simulations from the Hurricane Centers in the US. The National Hurricane Center (NHC) does have archives of operational Hurricane WRF (HWRF) runs for the past 5 to 6 years at a resolution of 9 km. However, the operational HWRF model has undergone significant changes every year since 2007. The model will be upgraded to 3 km resolution for the 2012 season. NHC has three years of retrospective runs from 3 km HWRF that were evaluated and shown about 10 – 15% improvement over the operational HWRF runs at 9 km resolution.

Data of 5 to 6 years are in fact not long enough for a good estimation of the 50-year wind. The inconsistency in the model operation is another problem. One way to overcome these is to run the model ourselves. This requires a longer project and computer resources and is obviously beyond the scope of the current project.

However, it is of great value if we could have the possibility to simulate a few tropical hurricanes using WRF and eventually HWRF. One of the purposes is to find how the WRF and HWRF hurricanes behave and how well they can be simulated. Another purpose is to examine the statistical method of Ott (2006) using the 2D and 3Dwind fields from the mesoscale weather model.

6.3 Extreme winds from Monte Carlo simulation based on best track data.

Following Annex J (IEC 2014), a tropical cyclone of relevance for a given site is considered to be characterized by six parameters: The occurrence rate within a radius of 500 km from the sites is denoted Λ . It must be determined from year(s) of data as available. Additionally its translation speed is denoted C, and

the approach angle, θ, measured counter clock wise from East; finally the minimum approach distance, denoted d_{min}. Two additional parameters are specified: R_m, the radius of maximum winds, the pressure depression, $\Delta p = p_\infty - p_C$, the difference between the external pressure and the center pressure, p_C, p_∞ is taken as 110 hPa, if not reported (ott,2006)

$$(6\text{-}3) \qquad \frac{p(r) - p_C}{p_\infty - p_C} = \exp(-\frac{R_m}{r})$$

The function in (6-3) can be formulated in terms of wind speed as presented in Figure 3.-1, denoted as the Holland curve from Ott (2006). In the Annex J(IEC, 2014), it is referred to Schloemer (1954).

In the following, we shall describe an approach to derive statistics of for Hurricanes, using Monte Carlo simulations based on the distributions of hurricane parameters derived from the observations of the six characteristic parameters, as described above. Based on Annex J From IEC (2014), and Ishihara et al (2005) the distribution functions for these parameters are estimated empirically as follows in Table 6.-1. Various data bases exist for available hurricane climatology, see e.g. section 5 or the DNV study report (DNV, 2011).

Neglecting Λ, the remaining five hurricane parameters to be considered are organized in vector form as follows, where the mean values have been subtracted, and the resulting parameters normalized by their standard deviation:

$$(6\text{-}4) \qquad \mathbf{X^T} = \left\{ \ln(\Delta p), \ln(R_m), \ln(C), \theta, d_{\min} \right\}$$

The parameters in (6-4) must be considered correlated within the data set available, consider e.g. a coastal region. The covariance matrix of $\mathbf{X^T}$ is denoted $\underline{\mathbf{S}}$. The eigen values, denoted $\lambda^{(k)}$ and the eigen vectors $\Phi^{(k)}$ are calculated from the following equation:

$$(6\text{-}5) \qquad [\mathbf{S} - \lambda^{(k)}\mathbf{E}]\mathbf{\Phi}^{(k)} = 0.$$

Here $\mathbf{E}$ is the unity tensor. The independent "orthogonal parameters" $\mathbf{Z}_i$, with five components, corresponding to $\mathbf{X_i}$, are found by expanding the parameters along the $\Phi^{(i)}$ eigen vectors.

$$(6\text{-}6) \qquad \begin{aligned} \mathbf{X}_i &= [\mathbf{\Phi}^k]^{-1}\mathbf{Z_i} \\ \mathbf{Z_i} &= [\mathbf{\Phi^k}]\mathbf{X}_i \end{aligned}$$

Here subscript i refers to each individual set of **X** as given by (6-4). Hence, from our multi- year hurricane observations we have obtained sets of **X**, characterizing each hurricane event. Correspondingly a set of orthogonal **Z**s are derived from (6-6). The individual **Z** components are orthogonal, assumed to mean uncorrelated, to each other within the set of observations, owing to (6-6). The distribution functions for **X** and **Z** are found empirically from the raw and the transformed data, respectively. We will understand the distribution $F(Xs)$ as the probability that $-\infty < X < Xs$ for all X , and correspondingly for the other parameters Z . For **Z** the distributions are fitted by a mixed probability function of a normal distribution and a uniform distribution (Ishihara et al, 2005). Based on a Monte Carlo variation of the uncorrelated **Z** parameters, one can now simulate many years of Hurricanes, first in terms of **Z** and subsequently by use of (6-6) in term of the **X** parameters.   The X distributions are fitted by the distribution functions described in table 6-1. If inclusion of the Monte Carlo simulated Z parameter cases modifies the **X**-distribution functions away from the empirical distributions found from the observations, it is recommended to modify the **X** such that the actual distribution functions approximate the empirical distribution functions of Table 6.-1. The methodology is illustrated in Figure 4 in Ishahara (2005), where the modification of **X** from the simulated **Z**s is achieved by a slight change in one of the correlation coefficients.

Table 6.-1. Summary of distribution functions fitted to the hurricane parameters

Parameter	Distribution
Frequency of occurrence, Λ	Poisson Distribution
Minimum distance, d_{min}	Quadratic function Distribution
Approach Angle, θ	Normal distribution
Depression, Δp	Mixed LogNormal-Weibul Distribution, MLNWB
Radius Max Wind, Rm	MLNWB
Translation speed, C	MLNWB
Orthogonal transformed parameters, Z, eq 0-4	Mixed Normal and Uniform distribution

The distributions of Table 2.6.-1 can be estimated from the observations available, denoted **X**. as well for the derived orthogonalized uncorrelated variables, denoted, **Z**. Additionally, the correlations between the different parameters must be estimated, to orthogonalise the **X** -parameters into the **Z**-parameters , before a Monte Carlo simulation can be enacted. A modified orthogonal decomposition method (MOD) is suggested. The Monte Carlo method is implemented as illustrated in Figure 6-4.: For a given hurricane, each

of the 5 uncorrelated Z parameters are varied randomly, and its associated distribution F(Z) attain the associated values.

As to the correlations **S**, there is some ambiguity between Ishahara(2005) and IEC(2014). The first defines the **X** as ($\triangle$p, Rm, C, θ, d_{min}), which is different from (6-4), where the logarithm has been applied on the first 3 of these variable. Both possibilities of course exist, and the difference may be ascribed to a time development of Ishahara's ideas. However, table 4 in Ishahara (2005) clearly indicates the components of **X** have to have their mean values subtracted and being normalized by their respective standard deviations. Ishahara (2005) includes a number of examples on the distribution function adaptations.
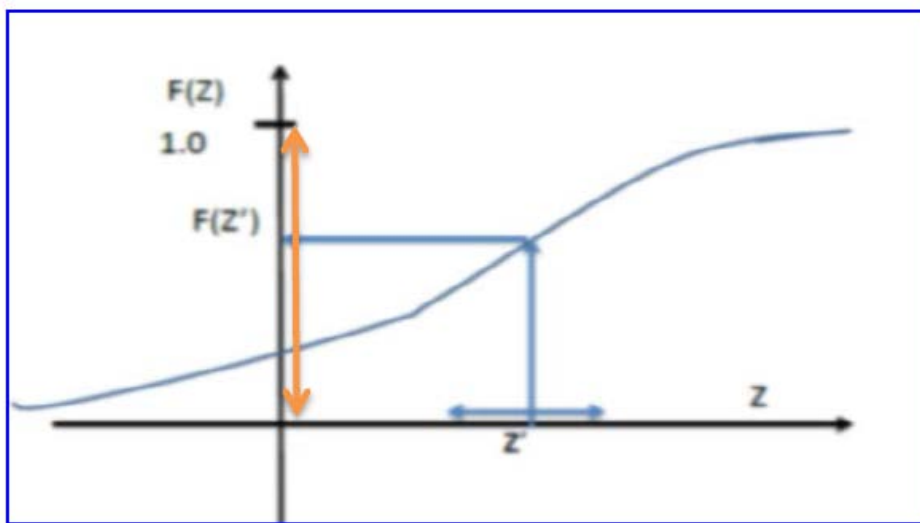

Figure 6-4 Implementation of the Monte Carlo system for the variable, **Z**, with the distribution F(Z). The random variation of F(Z') as a random number between zero and 1 is indicated by the red <-->. The corresponding Z' value for each F(Z') is found from the F(z) function as indicated by the blue lines.

6.3.1 Winds associated with the Hurricane parameters

The winds at a point ($\mathbf{x}_0$) over a flat homogeneous terrain (e.g. water) can be expressed as (6-7). The cyclone induces a gradient-wind speed $u_g(\mathbf{x}_0)$ and a flow angle $θ_g(\mathbf{x}_0)$. This flow can be considered the balance between the pressure gradient force, the Coriolis force and the centrifugal forces (as given by (3-1), overlaid by the translation speed and direction of the cyclone (C, θ). From Ishihara et al (1995), one obtains:

(6-7)
$$u_g(\mathbf{x}_0) = \left(\frac{-C\sin(\varphi-\theta)-fr}{2} \right) + \sqrt{(\frac{-C\sin(\varphi-\theta)-fr}{2})^2 + \frac{r}{\rho}\frac{\partial p(r)}{\partial r}};$$

$$\theta_g(\mathbf{x}_0) = \pi - \varphi$$

Elements of extreme wind modeling for hurricanes

Here r is the distance from the center of the hurricane of our site point ($\mathbf{x}_0$) and φ the angle between the site position and the hurricane center, measured counter clock wise from East. ($u_g(\mathbf{x}_0)$, $\theta_g(\mathbf{x}_0)$) varies with time as the hurricane moves. A time variation of ($u_g(\mathbf{x}_0)$, $\theta_g(\mathbf{x}_0)$) can be modeled, assuming the hurricane track is linear described by the approach angle θ and the translation speed C. Hereby time histories can be extracted and the maximum loading wind speed estimated for each of the hurricanes can be included in the statistical set of hurricane data.

The winds at hub-height depend on u_g and the wind profile from the ground and up. For homogenous terrain Ishahara (2005) provide and semi empirical form for both angle and speed as function of height, z. But other profile expressions can be considered as well. For inhomogeneous terrain (coastal), CFD, mesoscale modeling or other type formulation can be applied, e.g linear models of the WASP -type.

6.3.2 Applications.

The Monte Carlo simulation serves to simulate hurricane events ad infinitum that all follow the probability structure, characterizing the observations.
Using the approach in Figure 6-4, we can simulate a hurricane characterized by parameters chosen from the Monte Carlo simulations. The probability of occurrence is described by:

(6-8)   F(**Z**) =F0(Λ)*F1(Z1)*F2(Z2)*F3(Z3)*F4(Z4)*F5(Z5)
         =F(**X**) = (Λ, X1, X2,X3,X4,X5)

where we have introduced the distribution for the occurrence rate, Λ. Here we used that the **Z**-variates are considered independent.
From (6.7) we can now obtain the wind distribution at our site, point ($\mathbf{x}_0$), from the simulated hurricane, using appropriate profile functions through the boundary layer. Hereby various distribution functions for various aspects of hurricane winds can be constructed.

6.3.3 Extreme distribution of mixed climates

Extreme winds can be determined from Gumbel distributions:

$$G(U_i) \approx 1 - iT_0 / T = \exp(-\exp(\frac{U_i - \beta}{\alpha}))) \rightarrow$$

(6.-9)

$$U_i = \beta - \alpha \ln(-\ln(1 - \frac{iT_0}{T})) \approx \beta + \alpha \ln(\frac{T}{iT_0})$$

Here $G(U_i)$ means the probability that $U < U_i$. T is some long time, i.e. 50-100 years, T_0 is the basic time for which the maximum value is sampled, for example one year. G(U) is the distribution for the sequence of maximum values recorded/modelled every T_0. β is the most probable value, while α is a measure of the standard deviation for a Gumbel distribution. Subscript i refers

to the number in a size ranking list of U. Notably, with i=1, we have the highest probable value during time T.

The Gumbel distribution can be (and is) used for the non-hurricane weather as well, subscript nh, and for the hurricanes, subscript h. Following Ishahara we assume that the event are independent of each other, meaning that the combined Gumbel, $G_c(U) = G_{nh}(U) * G_h(U)$. Here the $G_{nh}(U)$ must be extrapolated from data , while $G_{nh}(U)$ can be plotted directly from the Monte Carlo simulations of simulations of hundreds of years of simulated hurricanes, assuming the overall distributions to be unchanged.

From (6-9) is seen that the relation between the maximum wind speed U and the time ratioT_0/T is derived by taking the logarithm of the distribution. Doing so we see that $\ln(G_c) = \ln(G_{nh}) + \ln(G_h)$, and the result will then depend on the behavior of the α and β for the two types of distribution functions. Also here various modifications to the Gumbel distributions can be used.

7. Discussion.

An important difference between the extreme winds for hurricanes and the similar extreme winds for mid-latitude storms as considered in Europe is that the European estimates are transparently derived from directly measured or modelled wind data; while less direct wind climatology is available for hurricanes, given the scarcity of the event at a given location and its severity, when it happens. Instead one has series of best tracks with associated pressure depressions and other supplementary data, allowing one to estimate the maximum wind from a (perhaps dubious) correlation to the pressure depression. Not all of the data sets contain information enough for a fuller description of the hurricane, and most often size information is missing. Additionally to this there are a number of observed and modelled wind data that so far do not have direct bearing on establishing the extreme wind climatology for hurricanes. Hence both the maximum wind and the size of the hurricane are estimated with an uncertainty that is difficult to quantify. To this must be added that discrepancies exist between best track data from different agencies. The data are also inhomogeneous in the sense that methods have evolved over the years. All this adds to the uncertainty of extreme wind estimation, see discussion in Ott (2006).

One aspect of extreme value estimation is similar for Mid-latitude frontal winds and hurricane winds, application of Gumbel formalisms to extract the extreme (and therefore low probability) wind estimates for the shorter time series.

We report two methodologies for this estimation technique, both being based on the "best track hurricane observations" with a Holland(1980) type model for the wind variation around the pressure depression : The direct method, see section 6.1, applied by Ott (2006) is the simplest and focus directly on the maximum winds from the cyclones for open water surfaces. The other method, see section 6.3, is recommended by IEC(2014) and has been in use for coastal regions, applying both physical modelling of the wind profile in the lower atmosphere, and statistical methods involving decorrelations of the governing parameters, and Monte Carlo simulation to "artificially extend " the observation period.

It should be pointed out that a number of buoy sites on the US East Coast, in regions where the extreme winds are hurricane determined. Here multiyear records are long enough, up to more than 10 years, for application of Gumbel estimation of the 50 and 100 year values of wind and wave height to be employed (ABS, 2011, p 34).

In section.6-2, we have described a future-maybe near future-, possibility of using numerical modelling based on various reanalysis data, to derive directly a climatology for hurricane winds using spectral correction to correct for the lack of resolution. When this methodology reach maturity, it may be used either separated or in conjunction with the observational following of hurricanes, taking most of the space in this note.

Additionally we have discussed the turbulence structure associated with hurricanes and sketched how to introduce this turbulence into the modelling.

Finally, we must admit that the report misses and important aspect of hurricane weather: The structure and the impact of the surface waves, associated with the hurricane winds. This issue will have to be referred to other sources.

References

American Bureau of Shipping, ABS (2011) Design standards for offshore wind farms. 211pp

American Petroleum Institute, API (2007) *API Bulletin 2INT-MET*. Interim Guidance on Hurricane conditions in the Gulf of Mexico.

Balderrama J.A., Masters F.J., Gurley, K.R. (2012): Peak factor estimation in hurricane surface winds. *J.Wind Engin. Indust. Aerodyn.* **102**, 1–13.

Dimitrov N K, Natarajan A, and M Kelly (2015). Model of wind shear conditional on turbulence and its impact on wind turbine loads. *Wind Energy* **18**(11), 1917–1931.

DNV Denmark(2011). Recommended practise for wind turbines in hurricanes. *DNV report PP022568-01*. Confidential.

Emanuel K (2004);   Tropical Cyclone Energetics and Structure. In *Atmospheric Turbulence and Mesoscale Meteorology*, E. Fedorovich, R. Rotunno and B. Stevens, editors, Cambridge University Press, 280 pp.

Emanuel K, and T Jagger (2010); "On estimating hurricane return periods." *J. Appl. Meteor. Clim.*, **49**, 837-844.

Franklin, J, Black M and K Valde (2000) Eyewall wind profiles in hurricanes determined by GPS dropsondes. Proc. 24th Conference Hurricanes and Tropical Meteorology, AMS, 448-449.

French JR, Drennan WM, Zhang JA, Black PG (2007); "Turbulent fluxes in the hurricane boundary layer.

part 1: Momentum flux." *J.Atmos.Sci.* **64**, 1089-1102.

International Electrotechnical Commission, IEC, (2009) IEC 61400-3: Wind turbines-Part 3: Design requirements for offshore wind turbines.

Holland, G.(1980) An analytic model of the wind and pressure profiles in hurricanes. Mon. Wea. Rev. 108, 1212-1218l

IEC (2014)International Electrotechnical Commission, IEC, (2014) IEC 61400-1 Ed.4: Wind turbines –Part 1: Design requirements. 152 p. Annex J (Informative) Prediction of extreme wind speed of tropical cyclones by using Monte Carlo Simulation method. 125-129

Ishihara, T, Siang, KK, Leong, CC, Fujino, Y (2005) Wind field model and mixed probability distribution function for typhoon simulation. The Sixth Asia-Pacific Conference on Wind Engineering (APCWE-VI) Seoul, Korea, September 12-14, 2005, 412-426.

Ishihara, T, Matsui M, K Hibi (1995) An analytical model for simulation of the wind field in a typhoon boundary layer. J. Wind Eng. Ind Aerodyn. **13**, 139-152.

Kaimal JC, Wyngaard JC, Izumi Y, Coté OR (1972); "Spectral characteristics of surface-layer turbulence." *Q.J.R. Meteorol. Soc.* **98**, 563-598.

Kareem A, Zhao J (1994): "Analysis of non-Gaussian surge response of tension leg platforms under wind loads." *J.Offshore Mech. Arctic Engin.* **116**(3),137–144.

Kristjansen, J.E, and E.W.Kolstad , eds. (2011) Special Section : IPY-THORPEX, Q.J.R. Meteorol. Soc. **137**, 1657-1790.

Larsén et al. (2011) Recipes for correcting the impact of effective mesoscale resolution on the estimation of extreme winds*, Journal of applied meteorology and climatology,* Doi:10.1175/JAMC-D-11.090, vol 51, No. 3, p521-533

Larsén X. and A. Kruger, 2014: Application of the spectral correction method to reanalysis data in South Africa, *Journal of wind engineering and industrial aerodynamics.* 133 (2014) 110-122.

Larsén, X.G.,KrugerA.,Badger,J.,Jørgensen,H.,2013a.Extremewindatlasesof South Africafromglobalreanalysisdata.In:ProceedingsoftheScientific Proceedings(online).European–African ConferenceofWindEngineering, Cambridge, UK.

Larsén X., Badger J., Hahmann A. N. and Mortensen N.G. 2013b: The selective dynamical downscaling method for extreme wind atlases, *Wind Energy*, **16**:1167–1182, DOI:10.1002/we.1544.

Lorsolo S, Zhang JA, Marks F, Gamache J. (2010); "Estimation and mapping of hurricane turbulent energy using airborne Doppler measurements." *Mon. Weather Rev.* **131**, 3656-3670.

Makin, V. K. (2005) A note on the drag of the sea surface at hurricane winds. Boundary Layer Meteorology, 115, 169-175.

Mann J (1994); "The spatial structure of neutral atmospheric surface-layer turbulence." *J.Fluid Mech.* **273**, 141-168.

Mann J (1998); "Wind field simulation." *Prob. Engin. Mech.* **13**, 269-282.

Ott, S. (2006) Extreme Winds in the Western North Pacific. Risø-R-1544(EN).

Peña A, Gryning S-E, Mann J (2010); "On the length-scale of the wind profile." *Q.J.R. Meteorol. Soc.* **136**, 2119-2131.

Rasmussen, E. A. and J. Turner (2003) Polar Lows. Cambridge University Press.

Schloemer, RW (1954) Analysis and synthesis of hurricane wind patterns over Lake Okkchobee in Florida, Hydrometeorological Report No. 31

Smith, R. K. and M.T. Montgomery (2010) Hurricane boundary layer theory. Q.J. Roy Met Soc., 136, 1665-1670.

Smith, R.K. and G. L. Thomsen (2010)" Dependence of tropical-cyclon intensitification on the boundary-layer representation in a numerical model". Q. J. Roy Met Soc., 136, 1671-1685.

Vickery, P.J. and P.F. Skerlj (2005); "Hurricane Gust Factors Revisited." *J. Struct. Engin.***131**, 825-832.

Wang B, Hu F, Cheng X (2011); "Wind gust and turbulence statistics of typhoons in South China." *Acta Meteor. Sinica*, **25**(1),113–127.

Wikipedia (Hurricanes, Tropical Cyclones)

Yu B, Chowdhury AG, Masters FJ (2008); "Hurricane Wind Power Spectra, Cospectra, and Integral Length Scales." *Boundary-Layer Meteorol.* **129**, 411-430.

Zhang J, Drennan WM, Black PB, French JR. *(*2009*); "*Turbulence structure of the hurricane boundary layer between the outer rainbands*." J. Atmos. Sci.* **66***: 2455–2467.*

Zhang, J. (2011) "Spectral characteristics of turbulence in the hurricane boundary layer over the ocean between rain bands." *Q.J.R Meteorol. Soc.* **136**, 918-926

([årstal]): [Titel på publikation], side [xx-xx], udkommet på [trykkeri/sted].

Acknowledgement

DTU Vindenergi er et institut under Danmarks Tekniske Universitet med en unik integration af forskning, uddannelse, innovation og offentlige/private konsulentopgaver inden for vindenergi. Vores aktiviteter bidrager til nye muligheder og teknologier inden for udnyttelse af vindenergi, både globalt og nationalt. Forskningen har fokus på specifikke tekniske og videnskabelige områder, der er centrale for udvikling, innovation og brug af vindenergi, og som danner grundlaget for højt kvalificerede uddannelser på universitetet.

Vi har mere end 240 ansatte og heraf er ca. 60 ph.d. studerende. Forskningen tager udgangspunkt i ni forskningsprogrammer, der er organiseret i tre hovedgrupper: vindenergisystemer, vindmølleteknologi og grundlag for vindenergi.